Published in final edited form as:

Biomaterials. 2015 September ; 64: 33–44. doi:10.1016/j.biomaterials.2015.06.026.

Matrix Rigidity Regulates the Transition of Tumor Cells to a Bone-Destructive Phenotype through Integrin β3 and TGF-β Receptor Type II

Jonathan M. Page[#1], **Alyssa R. Merkel**[#2,3,4], **Nazanin S. Ruppender**[1], **Ruijing Guo**[1], **Ushashi C. Dadwal**[1,3], **Shellese Cannonier**[2,3,5], **Sandip Basu**[6], **Scott A. Guelcher**[1,3,7], and **Julie A. Sterling**[2,3,4,5,*]

[1] Department of Chemical and Biomolecular Engineering, Vanderbilt University, Nashville, TN, 37235, USA

[2] Department of Veterans Affairs: Tennessee Valley Healthcare System, Nashville, TN, 37212, USA

[3] Center for Bone Biology, Vanderbilt University Medical Center, Nashville, TN, 37232, USA

[4] Division of Clinical Pharmacology, Department of Medicine, Vanderbilt University Medical Center, Nashville, TN, 37232, USA

[5] Department of Cancer Biology, Vanderbilt University Medical Center, Nashville, TN, 37232, USA

[6] Agilent Technologies, Chandler, AZ, 85226

[7] Department of Biomedical Engineering, Vanderbilt University, Nashville, TN, 37235, USA

[#] These authors contributed equally to this work.

Abstract

Cancer patients frequently develop skeletal metastases that significantly impact quality of life. Since bone metastases remain incurable, a clearer understanding of molecular mechanisms regulating skeletal metastases is required to develop new therapeutics that block establishment of tumors in bone. While many studies have suggested that the microenvironment contributes to bone metastases, the factors mediating tumors to progress from a quiescent to a bone-destructive state remain unclear. In this study, we hypothesized that the “soil” of the bone microenvironment, specifically the rigid mineralized extracellular matrix, stimulates the transition of the tumor cells to a bone-destructive phenotype. To test this hypothesis, we synthesized 2D polyurethane (PUR) films with elastic moduli ranging from the basement membrane (70 MPa) to cortical bone (3800 MPa) and measured expression of genes associated with mechanotransduction and bone metastases. We found that expression of Integrin β3 (*Iβ3*), as well as tumor-produced factors

[*] Corresponding author.

associated with bone destruction (*Gli2* and parathyroid hormone related protein (*PTHrP*)), significantly increased with matrix rigidity, and that blocking *Iβ3* reduced *Gli2* and *PTHrP* expression. To identify the mechanism by which Iβ3 regulates Gli2 and PTHrP (both are also known to be regulated by TGF-β), we performed Förster resonance energy transfer (FRET) and immunoprecipitation, which indicated that Iβ3 co-localized with TGF-β Receptor Type II (TGF-β RII) on rigid but not compliant films. Finally, transplantation of tumor cells expressing Iβ3 shRNA into the tibiae of athymic nude mice significantly reduced *PTHrP* and *Gli2* expression, as well as bone destruction, suggesting a crucial role for tumor-produced Iβ3 in disease progression. This study demonstrates that the rigid mineralized bone matrix can alter gene expression and bone destruction in an Iβ3/TGF-β-dependent manner, and suggests that Iβ3 inhibitors are a potential therapeutic approach for blocking tumor transition to a bone destructive phenotype.

Keywords

bone metastasis; mechanotransduction; matrix rigidity; parathyroid hormone-related protein; polyurethane; integrins; TGF-β

Introduction

Many of the most common tumors metastasize to bone, including breast, lung, and prostate cancer. It is estimated that 70% of breast cancer and 90% of prostate cancer patients with metastatic disease will develop bone metastases [1]. These metastases often develop years after the primary disease has been removed and are a major cause of morbidity and mortality [2, 3]. The primary clinical treatments for bone metastases focus on inhibiting bone resorption. While resorption inhibitors, like bisphosphonates, extend time to the first skeletal-related event, they neither directly inhibit tumor burden nor significantly extend survival when given after the diagnosis of a bone metastasis [4]. Thus, newer approaches are needed to improve patient outcomes [4], which require a mechanistic understanding of why some tumors establish in bone.

Recent evidence indicates that metastasis to bone and other organs can be predicted from the genes expressed by the primary tumor [5-9], but the mechanisms by which gene expression patterns and metastatic traits specific to bone transpire in tumor cells remains an unanswered question. A seminal study has shown that the breast tumor stroma contributes to the selection of invasive triple-negative (TN) breast cancer cells that are conditioned for metastasis to bone [10]. While this “metastasis seed pre-selection” mechanism affirms the role of the breast stroma to bestow an advantage for tumor cells to establish in bone, the factors mediating progression of the tumor cells from the pre-osteolytic to the osteolytic phase are unknown [11]. When metastatic tumor cells establish in bone, they secrete parathyroid hormone-related protein (PTHrP), interleukin 6 and 8, and/or other factors that induce osteoblast expression of Receptor Activator of NF-κβ Ligand (RANKL) [12, 13]. The consequent stimulation of osteoclast-mediated bone resorption results in release of TGF-β and other growth factors from the extracellular matrix that continues to drive the expression of PTHrP by the tumor cells [14, 15], which is regulated by the transcription factor Gli2 [14]. However, it is still unclear how bone microenvironmental effects on TGF-β

signaling regulate gene expression in tumor cells or why tumors recur in the bone many years after the primary tumor has been removed. More clearly understanding the events that induce progression from a pre-osteolytic to an osteolytic phenotype may allow clinicians to better predict which tumors may form bone metastases and may allow for improved treatments.

The mineralized extracellular matrix, which has an elastic modulus ranging from 10^3 – 10^6 kPa [16] differentiates bone from other tissues. Expression of *Gli2* and *PTHrP* by tumor cells *in vitro* correlates with bone-like matrix rigidity, which has been attributed to cross-talk between TGF-β and Rho-associated kinase (ROCK) [16-18], a factor regulating cell contractility [19]. Integrin-mediated cell-matrix interactions generate an adhesion molecule-integrin-actomyosin complex that can be shifted between inactive and signaling states by activation of myosin II or matrix rigidity [20]. However, recent studies suggest that rigidity-mediated changes in gene expression are driven by uniform displacements (100 – 150 nm) of the matrix [21-23]. Considering that cells cannot generate displacements > 100 nm on substrates more rigid than 10 – 100 kPa [21], 100 kPa been proposed as the upper limit at which cells enter a state of isometric contraction and cannot respond to further changes in rigidity [24]. Thus, the previously reported correlations of tumor cell proliferation [25], invasiveness [25], and expression of bone metastatic genes [16] with rigidity over ranges comparable to mineralized bone (10^3 – 10^6 kPa) cannot be explained by uniform displacements of the matrix. These observations raise questions regarding the mechanisms by which matrix rigidity regulates tumor cell gene expression in the mineralized bone microenvironment.

We hypothesized that when tumor cells become established in bone, the “soil” of the bone microenvironment, which is >10^3 more rigid than the primary site, stimulates their transition from the pre-osteolytic to the osteolytic phase. We further postulated that the transition to the osteolytic phenotype on substrates with bone-like rigidity is mediated by integrins, but not by uniform displacements of the matrix as reported previously [21-23] due to its high rigidity (> 100 kPa). TGF-β Receptor type II (TGF-β RII) interacts physically with β3 integrin sub-unit (Iβ3) to enhance TGF-β-mediated stimulation of MAP-kinases (MAPKs) during epithelial-mesenchymal transition (EMT) of mammary epithelial cells (MECs) [26]. However, the role of matrix rigidity in promoting interactions between these receptors has not been explored. We used a 2D polyurethane (PUR) film monoculture system to design matrices with rigidities ranging from that of the basement membrane to cortical bone, which is far more rigid than previous studies have examined. *In vitro* studies demonstrated that *Iβ3* expression correlated with bone-like rigidity, which led to co-localization of Iβ3 with TGF-β RII and increased expression of *PTHrP*. Inhibition of tumor-produced Iβ3 by molecular and genetic interference decreased expression of *PTHrP* and *Gli2 in vitro* and reduced bone destruction *in vivo*. These observations provide evidence for a previously unexplored mechanism by which crosstalk between solid-state and soluble factor signaling switches on osteolytic signaling in tumor cells.

Materials and Methods

Materials

Lysine diisocyanate (LDI) was purchased from Kyowa Hakko (New York, NY). Glycerol, stannous octoate, and ε-caprolactone were purchased from Sigma-Aldrich (St. Louis, MO). Glycolide and DL-lactide were supplied by Polysciences (Warrington, PA). COSCAT 83 bismuth catalyst was acquired from Vertullus (Hopewell, VA). Fibronectin (Fn) was purchased from Life Technologies (Grand Island, NY). The human breast cancer cell line, MDA-MB-231 was originally purchased from ATCC and a bone-tropic clone was generated by our laboratory [27]. The human squamous lung cancer cell line, RWGT2, was derived as previously described [28]. The human adenocarcinoma cell line, PC3 was purchased from ATCC. Dulbecco's Modification of Eagle's Medium (DMEM), Minimum Essential Medium α (α-MEM), and RMPI media were supplied by Mediatech (Manassas, VA). All media was supplemented with 10% Fetal Bovine Serum (Atlas, Fort Collins, CO) and 1% Penicillin and Streptomycin (Mediatech).

Synthesis of 2D Substrates for Cell Culture Experiments

2D films with varying rigidity were prepared for the cell culture experiments. The parameter typically used to quantify the rigidity of tissues and synthetic matrices is the elastic modulus, which is defined by the initial slope of the stress (σ) versus strain (ε) curve. Poly(ester urethane) (PUR) substrates were synthesized and characterized as described previously [29]. Briefly, an appropriate amount of poly(ε-caprolactone-co-glycolide) triol (Mn = 300, 600, 720 or 3000 g/mol) was mixed with an LDI-PEG prepolymer and COSCAT 83 catalyst (Vertellus) for 20s in a Hauschild SpeedMixerTM DAC 150 FVZ-K vortex mixer (FlackTek, Inc, Landrum, SC) (Figure 1A). The targeted index (ratio of NCO to OH equivalents times 100) was 105. The resultant mixture was poured into the wells of a tissue culture plate and allowed to cure for 24h at 60°C.

Measurement of Elastic Modulus by Nanoindentation

Nanoindentation measurements were performed as shown in Figure 1B-E to determine the Young's modulus of the substrate (E_s) by the method of Oliver and Pharr [30]. The reduced modulus E_r was calculated from load-displacement data acquired in the nanoindentation measurements:

$$E_r = \frac{\sqrt{\pi}}{2}\frac{S}{\sqrt{A}} \quad (1)$$

where A is the indenter contact area and the stiffness S is calculated from the initial slope of the unloading curve. The Young's modulus of the substrate E_s is related to the reduced modulus, the Young's modulus of the diamond indenter (E_i = 1141 GPa) and the Poisson ratios of the indentor (ν_i = 0.07) and the PUR substrate (ν_s = 0.5):

$$\frac{1}{E_r} = \frac{(1-v_s^2)}{E_s} + \frac{(1-v_i^2)}{E_i} \quad (2)$$

The Young's moduli of the PUR films (E_s) used in this study as obtained by nanoindentation are listed in Figure 1E.

Fibronectin Adsorption

To facilitate cell adhesion and ensure that the surface chemistry was constant for all substrates tested, fibronectin (Fn) was adsorbed to the surface of the substrates by incubation in a solution of Fn in PBS (0.5 – 50 4 μg/mL) at 4°C overnight. Coated substrates were incubated in a solution of Fn antibody (1:1000) followed by incubation with a secondary HRP-conjugated antibody to measure the surface concentration of Fn. The relative amount of adsorbed antibody was then quantified by reaction with 2'- azino-bis(3-ethylbenzthiazoline-6-sulphonic acid) (ABTS) and subsequent optical density reading at 405nm. With the exception of the Fn dose response experiment (Figure 2E), PUR scaffolds were treated with 4.0 μg cm^{-3} Fn.

Tissue Culture

MDA-MB-231 cells were maintained in DMEM, RWGT2 cells in α-MEM, and PC3 cells in RPMI media. All media was supplemented with 10% FBS and 1% Penicillin and Streptomycin. To overexpress *Iβ3*, MDA-MB-231 cells were stably transfected with an *Iβ3* overexpressing plasmid (Obtained from Addgene from Dr. Timothy Springer, Boston Children's Hospital [31]) using lipofectamine and plus reagent (Life Technologies) per manufacturer's instructions. To inhibit *Iβ3*, MDA-MB-231 cells were stably transfected with a targeted shRNA (Santa Cruz) or a control plasmid (Santa Cruz) using an shRNA transfection reagent (Santa Cruz) per manufacturer's instructions. All cells were cultured at 37°C with 5% CO_2.

Drug Treatments

For Iβ3 signaling experiments, cells were treated with the αvβ3 antibody LM609 (EMD Millipore) at 10ug/mL or control antibody 12CA5 (Vanderbilt Antibody Core), the RGD-mimicking peptide Cilengitide (Selleckchem) at 10μM, the actin-myosin inhibitor Blebbistatin (Sigma) at 50μM, and the src stimulating peptide Bombesin (Sigma) at 20nM or DMSO control for 24 hours under normal culture conditions. For TGF-β signaling experiments, cells were treated with 5ng/mL recombinant human TGF-β1 (R&D) or buffer (5% BSA-HCl), Smad 3 phosphorylation inhibitor SIS3 (EMD Millipore) at 10μM, or the p38 MAPKα inhibitor SB202190 (Tocris) at 10μM for 24 hours under normal culture conditions.

Quantitative Real-time PCR

To measure changes in gene expression, mRNA reverse transcription was carried out using the qScript cDNA synthesis kit (Quanta, VWR) per manufacturer's instructions. Briefly, cells were harvested with trypsin after 24 hrs in culture and total RNA was extracted using the RNeasy Mini Kit (Qiagen). The qScript cDNA supermix was used to synthesize cDNA using 1μg total RNA. The expression of *PTHrP*, *Gli2*, *Iβ3* and *TGF-β RII* was measured in triplicate by quantitative qRT-PCR using validated TaqMan primers with the 7500 Real-Time PCR System (Applied Biosciences) using the following cycling conditions: 95°C for

15 seconds and 60°C for 1 minute, preceded by an initial incubation period of 95°C for 10 minutes. Quantification was performed using the absolute quantitative for human cells method using 18S as an internal control.

Western Blot Analysis

Cells were harvested 24 hrs after seeding on PUR substrates in a radioimmunoprecipitation buffer containing a cocktail of protease and phosphatase inhibitors (Pierce). Equal protein concentrations were prepared for loading with NuPAGE sample buffer (Life Technologies) and separated on a 10% SDS-PAGE gel (BioRad). Proteins were transferred to a PVDF membrane and blocked with 5% BSA in TBS containing 0.1% Tween-20 for 1h at room temperature, followed by incubation with either phospho-p38MAPK (1:1000, Cell Signalling), p38MAPK (1:1000, Cell Signalling), phospho-Smad2/3 (1:1000, Cell Signalling) or Smad2/3 (1:1000, Cell Signalling) antibodies overnight at 4°C. After washing, membranes were blotted with anti-rabbit IgG (1:2000, SantaCruz), and bands were detected by enhanced chemiluminescence using an In-Vivo MS FX Pro (Bruker). Membranes were then stripped and reprobed using an antibody for β-actin (1:5000, Sigma) as a loading control. Phosphorylated events were quantified by normalizing the band intensity of phosphorylated protein to total protein. Analysis was performed using Image J software.

Förster Resonance Energy Transfer (FRET) Microscopy

To investigate the association of TGF-β RII and Iβ3, we performed Förster Resonance Energy Transfer (FRET) and confocal microscopy. Briefly, the donor antibody (anti Iβ3 (SantaCruz)) was labeled with Alexa Fluor® 488 Carboxylic Acid, Succinimidyl Ester (Life Technologies) (Iβ3-488) and the acceptor antibody (anti TGF-β RII (SantaCruz)) was labeled with Alexa Fluor® 546 Carboxylic Acid, Succinimidyl Ester (Life Technologies) (TGF-β RII-546) in a 2.25:1 molar ratio of antibody:dye overnight at 4°. Labelled antibody was purified with size exclusion chromatography using PD-10 Desalting Columns (GE Healthcare). MDA-MB-231, RWGT2, and PC3 cells were grown on discs of rigid and compliant 2D PURs. After 24 hours of culture, cells were fixed with 10% Formaldehyde in PBS and stained overnight at 4° with Iβ3-488, TGF-β RII-546, Iβ3-488 + TGF-β RII-546 or IgG control (1ug/1×10^6 cells). FRET experiments were performed on a BioTek Synergy 2 plate reader using excitation filter 485/20 and emission filter 590/35. Data were subtracted from the fluorescence of IgG control. Representative images of MDA-MB-231 cells grown on glass coverslips were taken with a Zeiss LSM 510 inverted confocal microscope. Images were obtained for Iβ3-488 (ex: 488, em: BP 505-550), TGF-β RII-546 (ex: 543, em: BP 560-615), colocalization (merge) and FRET (ex: 488, em: LP 585).

Immunoprecipitation

To investigate association of membrane proteins, cells were lysed using a 1% Nonidet-P40 buffer containing a cocktail of protease and phosphatase inhibitors (Pierce). 400μg total protein lysate per tube was incubated overnight at 4°C under gentle end-over-end mixing with anti-TGF-βRII (1 μg, Santa Cruz). Subsequently, the immune complex was captured with protein A/G agarose resin, thoroughly washed with lysis buffer and eluted with non-reducing sample buffer. Proteins were then separated on a 10% SDS-PAGE gel (BioRad)

and transferred to a PVDF membrane. Following blocking with 5% milk in TBS with 0.1% Tween-20, membranes were incubated with anti-Iβ3 (Santa Cruz, 1:1000) or anti-TGF-β RII (Santa Cruz, 1:1000) at 4°C overnight. After washing, membranes were blotted with anti-rabbit or anti-mouse IgG (1:5000 Santa Cruz), and bands were detected by enhanced chemiluminescence using an In Vivo MS FX Pro (Bruker). The Iβ3 and TGF-βRII co-precipitation was quantified by normalizing the band intensity of Iβ3 pulled down with TGF-βRII to total protein (anti-TGF-βRII). Analysis was performed using Image J software.

Immunofluorescent Staining

MDA-MB-231-GFP cells were grown on rigid or compliant PUR films for 24 hours. Cells were fixed in 10% Formaldehyde and blocked in 3% BSA for 1 hour. Fixed cells were labeled with an anti-Focal Adhesion Kinase antibody (FAK, 1:800, Cell Signaling) overnight at 4°C. An Alexa Fluor® 546-tagged secondary antibody was used for detection of FAK. Images were obtained at 40× and 100× on an Olympus BX41 upright microscope. Cell area and FAK area were measured by ROI measurements using Metamorph Image analysis software.

Animal Study

MDA-MB-231 cells stably transfected with either a shβ3 or shControl plasmid (SantaCruz) were injected into the tibia of 4-6 week old athymic nude mice (Harlan). Tumor progression was monitored by weekly x-ray imaging on a XR-60 digital radiography system (Faxitron) at 35kVp for 8 sec. Mice were sacrificed at 25 days post tumor cell inoculation and hindlimbs were harvested for *ex vivo* analysis. Bone volume was assessed by micro-computed tomography analysis using a Scanco μCT 40 (Scanco Medical) at 70kVp and 125mA with a 12μm voxel size and an integration time of 300ms. Histomorphological analysis was performed on 4μm thick decalcified, paraffin-embedded sections. Hematoxylin and Eosin staining was used to evaluate tumor burden. All animal studies were performed in compliance with the Vanderbilt University Institutional Animal Care and Use Committee and the National Institutes of Health guidelines.

Statistical analysis

All statistical analyses were performed using InStat version 3.03 software (GraphPad Software, Inc.). Values are presented as mean ± SEM, and *P* values determined using unpaired *t* test, where *, $P < 0.05$.

Results

PTHrP, Gli2 and Iβ3 expression correlate with rigidity

PUR films coated with fibronectin (Fn) were utilized to analyze the gene expression of MDA-MB-231-bone (bone metastatic clone of the original breast tumor line), RWGT2 (bone metastatic lung)[28], and PC3 (bone metastatic prostate) cancer cells as a function of matrix rigidity. All cell lines are prone to metastatic invasion of bone and the consequent formation of osteolytic tumors. MDA-MB-231, RWGT2, and PC3 cells expressed significantly increasing ($p<0.001$) amounts of *PTHrP*, *Gli2*, and *Iβ3* as the substrate rigidity increased from basement membrane levels (2,000 – 70,000 kPa) to that of trabecular bone

(90,000 – 365,000 kPa) (Figure 2A-C). Gli2 protein expression also significantly increased (see Figure 1A of [32]). Furthermore, when imaged by scanning electron microscopy (SEM), MDA-MB-231 and RWGT2 cells showed a spread phenotype on the rigid substrate, while cells grown on the compliant substrates were smaller and less spread (Figure 2D). While integrin expression correlates with rigidity in breast tumors in mice [33], the modulus of the mammary fat pad in these previous studies was <1.5 kPa, which is 10,000 times less rigid than the PUR substrates shown in Figure 1. Interestingly, the expression of *Iβ1* and *Iβ5* in MDA-MB-231 cells does not change significantly with increasing substrate rigidity, indicating that the cells are interacting with the matrix primarily through Iβ3 (see Figure 1B-D in [32]). To confirm that changes in Iβ3 concentration were mediated by rigidity and not differences in fibronectin (Fn) surface concentration, Fn was adsorbed on PUR films prior to culture of MDA-MB-231 cells. We have previously reported that Fn surface concentration is a function of Fn solution concentration but relatively independent of the rigidity of the PUR film [16]. Thus, we treated rigid and compliant films with varying concentrations (0 – 50 μg/ml) of Fn to vary the surface concentration (Figure 2E). Using immunofluorescence, we measured the concentration of Iβ3 produced by cells cultured on the films. At Fn concentrations exceeding 0.5 μg/mL, there were no changes in Iβ3 concentration for cells cultured on rigid or compliant PUR films (Figure 2E). However, as expected there was a significant change in Iβ3 between cells grown on rigid and compliant films. Furthermore, when tumor cells were cultured on PUR films treated with other matrix proteins, such as vitronectin, type I collagen, or poly-L-lysine, there was no change in the gene expression of *Iβ3, PTHrP, and Gli2* as a function of rigidity (see Figure 2 in [32]). These observations suggest that a threshold concentration of Fn, a primary binding ligand for $\alpha_v\beta_3$, is required to activate integrin-mediated changes in gene expression in response to matrix rigidity.

To determine whether or not these integrin-mediated changes in gene expression at moduli >1.5kPa were a result of traction forces, we looked downstream of the mechanotransduction pathway at how focal adhesion kinase (FAK) and cell area change in response to rigidity. Immunofluorescent images of MDA-MB-231-GFP cells labeled with anti-Focal Adhesion Kinase (FAK) (Figure 2F-G) reveal increases in cell size and FAK area with respect to substrate rigidity. Additionally, a linear relationship is observed between FAK area and cell area with increasing modulus (Figure 2H). These results signify that the tumor cells can respond to mechanical stimuli at rigidities ranging from basement membrane to that of trabecular bone.

Iβ3 mediates expression of PTHrP and Gli2 by tumor cells

The effect of *Iβ3* expression on *PTHrP* and *Gli2* was investigated utilizing MDA-MB-231 cells. In one treatment group, cells were transfected with shRNA inhibiting *Iβ3* (shβ3 cells). MDA-MB-231 cells were also treated with an inhibitor of $\alpha_v\beta_3$ integrin (LM609 [34]) or an RGD-mimicking peptide (Cilegnitide [35]). All three methods of blocking integrin function or expression produced a significant decrease ($p<0.01$) in *PTHrP* mRNA (Figure 3A-C) and *Gli2* mRNA (Figure 3D-F), as well as Gli2 protein (see Figure 3A-C in [32]) compared to control groups, indicating that Iβ3 mediates *Gli2* and *PTHrP* expression in MDA-MB-231-bone cells. Furthermore, when RWGT2 and PC3 cells were treated with LM609 or

Cilengitide, PTHrP and Gli2 mRNA expression significantly decreased (see Figure 3D-G in [32])

Expression of PTHrP and Gli2 is mediated by integrin/matrix binding and activation of Src family kinases

To further analyze the effects of *Iβ3* expression on *PTHrP* and *Gli2* expression, MDA-MB-231 cells were transfected to either over-express *Iβ3* (OE β3 cells) or silence *Iβ3* (shβ3). OE β3 cells were shown to have increased *PTHrP* expression compared to mock-transfected control cells (see Figure 4A in [32]). Additionally, when cultured on rigid and compliant PUR films, the OE β3 cells showed no statistical difference in *PTHrP* gene expression (see Figure 4B in [32]). While shβ3 cells had significantly decreased *PTHrP* and *Gli2* (Figure 3A,D), there was no significant changes observed in a panel of genes important in tumor metastasis (see Figure 7B in [32]). Thus, the OE β3 and shβ3 cells were utilized as model cell systems with high and low integrin expression, respectively (see Figure 4C-D in [32]). When cultured on rigid and compliant PUR films and imaged with scanning electron microscopy, the OE β3 cells were larger and more spread than the shβ3 cells on both rigid and compliant substrates (Figure 4A). Binding of integrin $\alpha_v\beta_3$ to Fn activates Src family kinases, an early event which leads to bridging of integrins to the cytoskeleton, tensioning of the integrin-matrix catch bond, and consequent displacement events [20, 21]. To investigate the relative contributions of integrin/matrix binding and displacement events to rigidity-mediated changes in gene expression, OE β3 cells were treated with inhibitors of myosin II and ROCK, which are key regulators of cell contractility. MDA-MB-231 and OE β3 cells were treated with blebbistatin, a drug that blocks the myosin heads in a complex with low actin-binding affinity [36]. Treatment of OE β3 cells with blebbistatin did not change *PTHrP*, *Gli2*, or *Iβ3* gene expression, but treatment of MDA-MB-231 cells with blebbistatin decreased *PTHrP*, *Gli2* and *Iβ3* expression ($p<0.05$, Figure 4B-D). Interestingly, myosin inhibition with blebbistatin did not change FAK area in MDA-MB-231 cells or OEβ3 cells (Figure 4H-I)

In a related experiment, shβ3 cells were treated with bombesin, a Src stimulator that upon integrin activation induces bridging of integrins to the cytoskeleton through talin [21] as well as tyrosine phosphorylation of TGF-β RII [26]. Treatment with bombesin significantly increased *PTHrP*, *Gli2*, and *Iβ3* gene expression in MDA-MB-231 and shβ3 cells ($p<0.005$, Figure 4E-G). Taken together, these observations suggest that integrin activation regulates *Gli2* and *PTHrP* expression through Src-mediated phosphorylation of TGF-β RII.

Physical interactions between Iβ3 and TGF-β Receptor II (TGF-β RII) correlate with rigidity

During epithelial-mesenchymal transition (EMT), Iβ3 physically interacts with TGF-β RII followed by phosphorylation of TGF-β RII by Src [26]. However, EMT typically occurs at the primary site, where the matrix is 10,000-fold more compliant than the bone microenvironment. To test the hypothesis that interactions between TGF-β RII and Iβ3 correlate with rigidity, we probed the interactions between these plasma membrane proteins by Förster resonance energy transfer (FRET) analysis (Figure 5A). MDA-MB-231, RWGT2, or PC3 cells were incubated with antibodies for Iβ3 and TGF-β RII that were labeled with a fluorescent FRET pair (Alexa Fluor 488 and Alexa Fluor 546). The fluorescent signal from

IgG control antibodies labeled with the same FRET pair was subtracted from the signal for the Iβ3 and TGF-β RII antibodies to calculate the background-subtracted FRET response. MDA-MB-231, RWGT2, and PC3 cells induced a greater FRET response when cultured on substrates with bone-like rigidity than on compliant substrates ($p<0.05$, Figure 5F). Representative confocal images show colocalization and a FRET response of Iβ3 and TGF-β RII in the cell membrane (Figure 5B-E). Interestingly, TGF-β RII was not affected by rigidity, which is supported by our qRT-PCR results (see Figure 5A in [32][cite DIB]). These results were confirmed by immunoprecipitation for TGF-β RII, which demonstrated increased co-precipitation of TGF-β RII and Iβ3 on rigid compared to compliant substrates (Figure 5G). To ensure that the Fn coating was not affecting the expression of either FRET target, a dose-response analysis was conducted (see Figure 5B in [32]). The FRET signal did not increase appreciably on rigid substrates above the threshold concentration of 0.5 μg/mL. Thus Iβ3, which is expressed significantly more on substrates with bone-like rigidity, physically interacts with TGF-β RII on rigid substrates, resulting in elevated osteolytic gene expression.

Exogenous TGF-β stimulation of PTHrP and Gli2 is Iβ3-dependent

To investigate crosstalk between TGF-β signaling, which stimulates expression of *PTHrP* and *Gli2* [14], and Iβ3–mediated signaling, shβ3-transfected or LM609-treated MDA-MB-231 cells were cultured in serum-free media on rigid PUR films and treated with exogenous TGF-β. shβ3 cells showed significantly reduced *PTHrP* and *Gli2* ($p<0.01$, Figure 6A-B) mRNA expression even in the presence of exogenous TGF-β. Inhibition of Iβ3 with LM609 showed similar results in MDA-MB-231 bone ($p<0.01$, Figure 6C-D) and RWGT2 and PC3 cells (see Figure 6 in [32]). However, *Iβ3* expression was not affected by TGF-β stimulation (Figure 6E). Thus, both TGF-β and Iβ3 signaling are required for *Gli2* and *PTHrP* expression. Since TGF-β signaling in bone metastases can be mediated through Smad- or p38 MAPKα-dependent downstream signaling [37], we investigated whether one or both of these pathways is stimulated by interactions between Iβ3 and TGF-β RII in the presence of exogenous TGF-β. Western blot analysis revealed significant changes in expression and phosphorylation of p38 MAPKα (Figure 7A), but no significant difference in expression and phosphorylation of SMAD2/3 (Figure 7B) when MDA-MB-231 cells were cultured on rigid compared to compliant substrates. Inhibition of p38 MAPKα via SB202190 significantly decreased *PTHrP* and *Gli2* expression by quantitative qRT- PCR on rigid substrates ($p<0.05$), while the Smad inhibitor SIS3 significantly decreased PTHrP ($p<0.05$) but not *Gli2* expression on rigid substrates (Figure 7C-D). These observations suggest that physical interactions between Iβ3 and TGF-β RII in response to bone rigidity activate TGF-β signaling primarily through p38 MAPKα.

Inhibition of Iβ3 in MDA-MB-231 cells reduces bone destruction in vivo

Since inhibition of *Iβ3* with shRNA reduced the expression of factors associated with bone destruction *in vitro*, we reasoned that inhibiting *Iβ3* would slow the progression of tumor-induced bone disease *in vivo*. Considering that blocking *Iβ3* reduces metastasis [38], we chose to directly inject mice with MDA-MB-231 cells stably expressing shβ3 into the tibia to eliminate any potential effect on metastasis. *Ex vivo* analyses using CT (Figure 8A, C) and radiography (Figure 8G) demonstrated a reduction in bone resorption, as evidenced by

increased BV/TV (Figure 8E) and reduced lesion number (Figure 8G) for shβ3 cells compared to mock-transfected cells. Blocking *Iβ3* did not have a significant effect on tumor growth (Figure 8B, D, and F and see Figure 7 in [32]), but the control cells grew in the trabecular bone closet to the injection site, while the shβ_3 cells resulted in tumors in the marrow space. Previous studies have shown that blocking tumor-produced Iβ3 reduces metastasis [38] and that systemic delivery of the Iβ3 inhibitor Cilegnitide inhibits bone resorption in a mouse model of bone metastasis [35]. While these previous studies highlight the role of Iβ3 in bone metastasis, they do not address the question of how tumor cells become established in the bone microenvironment. The reduced bone resorption and dispersion of tumor cells in the marrow space associated with shβ3 cells points to a major role of tumor-produced Iβ3 in switching tumor cells from the pre-osteolytic to the osteolytic phase in the bone microenvironment.

Discussion

In soft tissue, the increase in the rigidity of the extracellular matrix surrounding the tumor activates integrins, which increases both mitogenic signaling through soluble factors and also tumor cell contractility through Rho/ROCK [39, 40]. Increased cell contractility further increases matrix rigidity, which drives a positive feedback loop that triggers malignant transformation in epithelial cells [39, 41] and in some cases TGF-β-dependent EMT [42]. However, the extracellular matrix in bone is several orders of magnitude stiffer than soft tissue and cannot be directly remodeled by tumor cells [43]. Thus, the previously observed increase in *Gli2* and *PTHrP* expression when metastatic tumor cells were cultured on substrates with bone-like rigidities [16] cannot be explained by this mechanical positive feedback loop associated with malignant transformation in soft tissue [39, 40]. In this study, we utilized 2D polymeric substrates with rigidities tunable from that of the basement membrane to cortical bone to investigate the mechanism by which matrix rigidity regulates gene expression in tumor cells that are metastatic to bone. On matrices with rigidity equal to or exceeding that of trabecular bone, both expression of Iβ3 as well as its co-localization with TGF-β RII increased, resulting in up-regulation of TGF-β signaling through p38MAPK and Smad 2/3 and consequent *Gli2* and *PTHrP* expression (Figure 9).

Previous studies of our own and others have reported that metastasis to bone [44] and increased *PTHrP* expression in response to matrix rigidity [16] are mediated by ROCK, which stimulates contractility through the substrate-Fn-αvβ3-actin-myosin II mechanically sensitive cassette [20, 39]. Consistent with these observations, blebbistatin significantly reduced contractility, *Iβ3*, *Gli2* and *PTHrP* expression in MDA-MB-231 cells but not in OEβ3 cells (Figure 4). Thus, it was not possible to de-couple the effects of Iβ3 expression and contractility, which represents a limitation of this study. Both *Iβ3* expression and FAK area increased with rigidity on substrates stiffer than 10 MPa, which suggests that the contractile forces exerted by the cells increase over the MPa range. Current evidence suggests that contractility-mediated mechanosensory events are driven by uniform displacements (100 – 150 nm) of the matrix [21-23]. Values ranging from 10 – 100 kPa have been proposed as the upper limit of matrix rigidity that can result in a displacement of 100 – 150 nm [21, 24]. On substrates > 100 kPa, cells have been suggested to be in a state of isometric contraction in which they cannot respond to further changes in rigidity.

Consequently, the observed increase in *Gli2* and *PTHrP* expression by tumor cells interacting with bone-like matrices stiffer than 10 MPa cannot be explained by the rigidity sensing cycle based on uniform displacements of the matrix. While previous studies have identified the mechanosensory role of Iβ3 for cells cultured on polyacrylamide hydrogels (<1 MPa) [23, 45, 46] our observations point to a role for tumor-produced Iβ3 in the regulation of bone metastatic genes in response to rigid matrices that cannot be displaced > 100 nm by cells. To our knowledge, the present study is the first to show that rigid substrates can alter soluble factor signaling through physical interactions between integrins and growth factor receptors.

Force-generating events that drive matrix displacement in the rigidity-sensing cycle occur downstream of integrin/matrix binding and consequent Src activation [21]. In the present study, *in vitro* analyses demonstrated that the increase in Iβ3 on rigid matrices resulted in greater co-localization with TGF-βRII up-stream of Src. Integrins have been reported to couple with growth factor receptors such as TGF-βRII [26] and HER2 [47], resulting in the activation of downstream signaling cascades through Src phosphorylation of downstream targets. In the present study, activation of Src in shβ3 cells by treatment with bombesin rescued the expression of *Iβ3*, *Gli2*, and *PTHrP*. This observation is consistent with previous studies reporting that Src activates phosphorylation of TGF-β RII after formation of the Integrin β3-TGF-β RII complex [26, 48].

Iβ3 has been associated with cancer-induced bone disease through its essential role in osteoclast function [49, 50] and metastasis to bone [38]. Here we show that *Iβ3* expression directly regulates tumor cell gene expression, and that inhibiting *Iβ3* in tumor cells blocks bone destruction by reducing the expression of tumor-derived factors like PTHrP. This suggests that integrin inhibitors could block establishment of tumors in bone by inhibiting both osteoclast activity and also the expression of tumor-derived factors. Two $\alpha_v\beta_3$ integrin inhibitors are currently in clinical trials for treatment of different cancers [51]. Cilengitide, a cyclic peptide that inhibits integrin signaling, has been evaluated in a Phase III clinical trial for glioblastoma, but ultimately did not alter glioblastoma progression [52, 53]. Alternatively, Etaracizumab, an $\alpha_v\beta_3$ integrin antibody, has shown promise in pre-clinical trials for metastatic melanoma and castration-resistant prostate cancer and is now in Phase II clinical trials [51]. Our data suggest that these inhibitors may be effective for blocking metastatic tumors from responding to the rigid bone matrix and secreting factors (like PTHrP) associated with their transition to the osteolytic phase. Coupled with their previously reported anti-angiogenic, anti-metastatic, and anti-osteoclast properties, integrin inhibition is a promising target for drug development. Importantly, our data indicate that integrin inhibition (Cilingitide and LM609) reduces gene expression in multiple tumor types, suggesting that it may be broadly applicable for inhibiting metastatic disease. Additionally, our data suggest that TGF-β inhibitors, which are also in clinical trials for use in cancer, may have similar effects at inhibiting the ability of the tumor to respond to the rigid mineralized bone matrix [54], and may in part explain positive pre-clinical results from using TGF-β inhibitors in bone metastatic disease [55, 56].

The metastasis seed pre-selection mechanism postulates that the breast stroma contributes to the selection of breast cancer cells conditioned for metastasis to bone [10]. However, once

tumor cells become established in bone, the factors mediating their transition from the preosteolytic to the osteolytic phase have not been elucidated [11]. In this study, we have shown that rigid, bone-like matrices stimulate expression of osteolytic factors *in vitro* through Iβ3 and TGF-β RII complexation, which activates p38MAPKα signaling (and partially Smad 2/3) through Src phosphorylation [26]. This subsequently induces expression of the osteoclastogenic factor *PTHrP* and its transcription factor *Gli2*. Taken together, these data significantly add to our understanding of how tumor cells respond to the rigid mineralized bone matrix, and may have broad implications for other tumor types that grow in bone and for non-tumor cells present in the bone. Understanding the mechanisms involved in the establishment of these metastases could ultimately lead to new targeted therapies to improve clinical outcomes. Furthermore, this study suggests that Iβ3 inhibitors, which are currently in clinical trials for several tumor types, may also inhibit tumor-induced bone disease.

Conclusion

Our results demonstrate the importance of the physical rigidity of the tumor microenvironment in the regulation of genes important in mediating bone destruction, such as PTHrP and Gli2. This regulation was mediated by physical interactions between Iβ3 and TGF-βRII, which induced MAPK and Smad-mediated signaling. These data suggest that the response to rigidity may influence bone metastatic tumor cells to transition from a quiescent state to a bone destructive state, therefore blocking the cell's ability to sense this rigidity presents a novel therapeutic opportunity. Importantly, Iβ3 inhibitors are currently used clinically for other diseases and may be a promising approach for preventing the progression of tumors residing in bone.

Acknowledgments

This work was supported by NIH grant CA163499 (to S.A.G. and J.A.S.), VA Merit Award 1I01BX001957 (to J.A.S.), and NSF grant DMR-1006558 (to S.A.G.).

References

1. Guise TA, Yin JJ, Taylor S, Kumagai Y, Dallas M, Boyce B, et al. Evidence for a causal role of parathyroid hormone-related protein in the pathogenesis of human breast cancer-mediated osteolysis. J Clin Invest. 1996; 98:1544. [PubMed: 8833902]
2. Braun S, Kentenich C, Janni W, Hepp F, de Waal J, Willgeroth F, et al. Lack of effect of adjuvant chemotherapy on the elimination of single dormant tumor cells in bone marrow of high-risk breast cancer patients. Journal of Clinical Oncology. 2000; 18:80. [PubMed: 10623696]
3. Mundy GR. Metastasis: Metastasis to bone: causes, consequences and therapeutic opportunities. Nat Rev Cancer. 2002; 2:584–93. [PubMed: 12154351]
4. Neville-Webbe HL, Coleman RE. Bisphosphonates and RANK ligand inhibitors for the treatment and prevention of metastatic bone disease. European Journal of Cancer. 2010; 46:1211–22. [PubMed: 20347292]
5. Chang HY, Nuyten DS, Sneddon JB, Hastie T, Tibshirani R, Sorlie T, et al. Robustness, scalability, and integration of a wound-response gene expression signature in predicting breast cancer survival. Proceedings of the National Academy of Sciences of the United States of America. 2005; 102:3738–43. [PubMed: 15701700]
6. Chiang AC, Massague J. Molecular basis of metastasis. The New England journal of medicine. 2008; 359:2814–23. [PubMed: 19109576]

7. Minn AJ, Gupta GP, Siegel PM, Bos PD, Shu W, Giri DD, et al. Genes that mediate breast cancer metastasis to lung. Nature. 2005; 436:518–24. [PubMed: 16049480]
8. van 't Veer LJ, Dai H, van de Vijver MJ, He YD, Hart AA, Mao M, et al. Gene expression profiling predicts clinical outcome of breast cancer. Nature. 2002; 415:530–6. [PubMed: 11823860]
9. Weigelt B, Glas AM, Wessels LF, Witteveen AT, Peterse JL, van't Veer LJ. Gene expression profiles of primary breast tumors maintained in distant metastases. Proceedings of the National Academy of Sciences of the United States of America. 2003; 100:15901–5. [PubMed: 14665696]
10. Zhang XH, Jin X, Malladi S, Zou Y, Wen YH, Brogi E, et al. Selection of bone metastasis seeds by mesenchymal signals in the primary tumor stroma. Cell. 2013; 154:1060–73. [PubMed: 23993096]
11. Guise TA. Breast cancer bone metastases: it's all about the neighborhood. Cell. 2013; 154:957–9. [PubMed: 23993088]
12. Powell GJ, Southby J, Danks JA, Stillwell RG, Hayman JA, Henderson MA, et al. Localization of parathyroid hormone-related protein in breast cancer metastases: increased incidence in bone compared with other sites. Cancer research. 1991; 51:3059–61. [PubMed: 2032246]
13. Southby J, Kissin MW, Danks JA, Hayman JA, Moseley JM, Henderson MA, et al. Immunohistochemical localization of parathyroid hormone-related protein in human breast cancer. Cancer research. 1990; 50:7710–6. [PubMed: 2253214]
14. Sterling JA, Oyajobi BO, Grubbs B, Padalecki SS, Munoz SA, Gupta A, et al. The hedgehog signaling molecule Gli2 induces parathyroid hormone-related peptide expression and osteolysis in metastatic human breast cancer cells. Cancer research. 2006; 66:7548–53. [PubMed: 16885353]
15. Yin JJ, Selander K, Chirgwin JM, Dallas M, Grubbs BG, Wieser R, et al. TGF-beta signaling blockade inhibits PTHrP secretion by breast cancer cells and bone metastases development. J Clin Invest. 1999; 103:197–206. [PubMed: 9916131]
16. Ruppender NS, Merkel AR, Martin TJ, Mundy GR, Sterling JA, Guelcher SA. Matrix rigidity induces osteolytic gene expression of metastatic breast cancer cells. PloS one. 2010; 5:e15451. [PubMed: 21085597]
17. Sterling JA, Guelcher SA. Bone structural components regulating sites of tumor metastasis. Current osteoporosis reports. 2011; 9:89–95. [PubMed: 21424744]
18. Guelcher SA, Sterling JA. Contribution of bone tissue modulus to breast cancer metastasis to bone. Cancer microenvironment : official journal of the International Cancer Microenvironment Society. 2011; 4:247–59. [PubMed: 21789687]
19. Amano M, Nakayama M, Kaibuchi K. Rho-kinase/ROCK: A key regulator of the cytoskeleton and cell polarity. Cytoskeleton. 2010; 67:545–54. [PubMed: 20803696]
20. Boettiger D. Mechanical control of integrin-mediated adhesion and signaling. Current opinion in cell biology. 2012; 24:592–9. [PubMed: 22857903]
21. Moore SW, Roca-Cusachs P, Sheetz MP. Stretchy proteins on stretchy substrates: the important elements of integrin-mediated rigidity sensing. Developmental cell. 2010; 19:194–206. [PubMed: 20708583]
22. Saez A, Buguin A, Silberzan P, Ladoux B. Is the mechanical activity of epithelial cells controlled by deformations or forces? Biophysical journal. 2005; 89:L52–4. [PubMed: 16214867]
23. Jiang G, Huang AH, Cai Y, Tanase M, Sheetz MP. Rigidity sensing at the leading edge through alphavbeta3 integrins and RPTPalpha. Biophysical journal. 2006; 90:1804–9. [PubMed: 16339875]
24. Discher DE, Janmey P, Wang YL. Tissue cells feel and respond to the stiffness of their substrate. Science. 2005; 310:1139–43. [PubMed: 16293750]
25. Kostic A, Lynch CD, Sheetz MP. Differential matrix rigidity response in breast cancer cell lines correlates with the tissue tropism. PloS one. 2009; 4:e6361. [PubMed: 19626122]
26. Galliher AJ, Schiemann WP. Beta3 integrin and Src facilitate transforming growth factor-beta mediated induction of epithelial-mesenchymal transition in mammary epithelial cells. Breast Cancer Res. 2006; 8:R42. [PubMed: 16859511]
27. Campbell JP, Merkel AR, Masood-Campbell SK, Elefteriou F, Sterling JA. Models of bone metastasis. Journal of visualized experiments : JoVE. 2012:e4260. [PubMed: 22972196]
28. Guise TA, Yoneda T, Yates AJ, Mundy GR. The combined effect of tumor-produced parathyroid hormone-related protein and transforming growth factor-alpha enhance hypercalcemia in vivo and

bone resorption in vitro. The Journal of clinical endocrinology and metabolism. 1993; 77:40–5. [PubMed: 8325957]

29. Ruppender NS MA, Martin TJ, Mundy GR, Sterling JA, Guelcher SA. Matrix Rigidity Induces Osteolytic Gene Expression of Metastatic Breast Cancer Cells. PLoS One. 2010; 5:e15451. [PubMed: 21085597]
30. Oliver WP, GM. An improved technique for determining hardness and elastic modulus using load and displacement sensing indentation. Journal of Materials Research. 1992; 7:1564–83.
31. Takagi J, Petre BM, Walz T, Springer TA. Global conformational rearrangements in integrin extracellular domains in outside-in and inside-out signaling. Cell. 2002; 110:599–11. [PubMed: 12230977]
32. Page JM, Merkel A, Ruppender N, Dadwal UC, Cannonier SA, Guo R, et al. Altering adsorbed proteins or cellular gene expression in MDA-MB-231 cells aeffects PTHrP and Gli2 without altering cell growth. Biomaterials. 2015 Submitted.
33. Levental KR, Yu H, Kass L, Lakins JN, Egeblad M, Erler JT, et al. Matrix Crosslinking Forces Tumor Progression by Enhancing Integrin Signaling. Cell. 2009; 139:891–906. [PubMed: 19931152]
34. Rucci N, DiGiacinto C, Orru L, Millimaggi D, Baron R, Teti A. A novel protein kinase C alpha-dependent signal to ERK1/2 activated by alphaVbeta3 integrin in osteoclasts and in Chinese hamster ovary (CHO) cells. Journal of cell science. 2005; 118:3263–75. [PubMed: 16014375]
35. Bretschi M, Merz M, Komljenovic D, Berger MR, Semmler W, Bauerle T. Cilengitide inhibits metastatic bone colonization in a nude rat model. Oncology reports. 2011; 26:843–51. [PubMed: 21725616]
36. Kovacs M, Toth J, Hetenyi C, Malnasi-Csizmadia A, Sellers JR. Mechanism of blebbistatin inhibition of myosin II. The Journal of biological chemistry. 2004; 279:35557–63. [PubMed: 15205456]
37. Yin JJ, Selander K, Chirgwin JM, Dallas M, Grubbs BG, Wieser R, et al. TGF-beta signaling blockade inhibits PTHrP secretion by breast cancer cells and bone metastases development. The Journal of clinical investigation. 1999; 103:197–206. [PubMed: 9916131]
38. Zhao Y, Bachelier R, Treilleux I, Pujuguet P, Peyruchaud O, Baron R, et al. Tumor alphavbeta3 integrin is a therapeutic target for breast cancer bone metastases. Cancer research. 2007; 67:5821–30. [PubMed: 17575150]
39. Huang S, Ingber DE. Cell tension, matrix mechanics, and cancer development. Cancer cell. 2005; 8:175–6. [PubMed: 16169461]
40. Paszek MJ, Zahir N, Johnson KR, Lakins JN, Rozenberg GI, Gefen A, et al. Tensional homeostasis and the malignant phenotype. Cancer cell. 2005; 8:241–54. [PubMed: 16169468]
41. Chaudhuri O, Koshy ST, Branco da Cunha C, Shin JW, Verbeke CS, Allison KH, et al. Extracellular matrix stiffness and composition jointly regulate the induction of malignant phenotypes in mammary epithelium. Nature materials. 2014
42. Brown AC, Fiore VF, Sulchek TA, Barker TH. Physical and chemical microenvironmental cues orthogonally control the degree and duration of fibrosis-associated epithelial-tomesenchymal transitions. The Journal of pathology. 2013; 229:25–35. [PubMed: 23018598]
43. Martin TJ, Mundy GR. Bone metastasis: can osteoclasts be excluded? Nature. 2007; 445:E19. discussion E-20. [PubMed: 17314931]
44. Liu S, Goldstein RH, Scepansky EM, Rosenblatt M. Inhibition of rho-associated kinase signaling prevents breast cancer metastasis to human bone. Cancer research. 2009; 69:8742–51. [PubMed: 19887617]
45. Schiller HB, Hermann MR, Polleux J, Vignaud T, Zanivan S, Friedel CC, et al. beta1-and alphav-class integrins cooperate to regulate myosin II during rigidity sensing of fibronectin-based microenvironments. Nature cell biology. 2013; 15:625–36.
46. Jones C, Ehrlich HP. Fibroblast expression of alpha-smooth muscle actin, alpha2beta1 integrin and alphavbeta3 integrin: influence of surface rigidity. Experimental and molecular pathology. 2011; 91:394–9. [PubMed: 21530503]

47. Wang SE, Xiang B, Zent R, Quaranta V, Pozzi A, Arteaga CL. Transforming growth factor beta induces clustering of HER2 and integrins by activating Src-focal adhesion kinase and receptor association to the cytoskeleton. Cancer research. 2009; 69:475–82. [PubMed: 19147560]

48. Galliher AJ, Schiemann WP. Src phosphorylates Tyr284 in TGF-beta type II receptor and regulates TGF-beta stimulation of p38 MAPK during breast cancer cell proliferation and invasion. Cancer research. 2007; 67:3752–8. [PubMed: 17440088]

49. Bakewell SJ, Nestor P, Prasad S, Tomasson MH, Dowland N, Mehrotra M, et al. Platelet and osteoclast beta3 integrins are critical for bone metastasis. Proceedings of the National Academy of Sciences of the United States of America. 2003; 100:14205–10. [PubMed: 14612570]

50. Schneider JG, Amend SR, Weilbaecher KN. Integrins and bone metastasis: integrating tumor cell and stromal cell interactions. Bone. 2011; 48:54–65. [PubMed: 20850578]

51. Goodman SL, Picard M. Integrins as therapeutic targets. Trends in pharmacological sciences. 2012; 33:405–12. [PubMed: 22633092]

52. Burke PA, DeNardo SJ, Miers LA, Lamborn KR, Matzku S, DeNardo GL. Cilengitide targeting of alpha(v)beta(3) integrin receptor synergizes with radioimmunotherapy to increase efficacy and apoptosis in breast cancer xenografts. Cancer research. 2002; 62:4263–72. [PubMed: 12154028]

53. Eisele G, Wick A, Eisele AC, Clement PM, Tonn J, Tabatabai G, et al. Cilengitide treatment of newly diagnosed glioblastoma patients does not alter patterns of progression. Journal of neuro-oncology. 2014; 117:141–5. [PubMed: 24442484]

54. Lonning S, Mannick J, McPherson JM. Antibody targeting of TGF-beta in cancer patients. Current pharmaceutical biotechnology. 2011; 12:2176–89. [PubMed: 21619535]

55. Biswas S, Nyman JS, Alvarez J, Chakrabarti A, Ayres A, Sterling J, et al. Anti-transforming growth factor ss antibody treatment rescues bone loss and prevents breast cancer metastasis to bone. PloS one. 2011; 6:e27090. [PubMed: 22096521]

56. Mohammad KS, Javelaud D, Fournier PG, Niewolna M, McKenna CR, Peng XH, et al. TGF-beta-RI kinase inhibitor SD-208 reduces the development and progression of melanoma bone metastases. Cancer research. 2011; 71:175–84. [PubMed: 21084275]

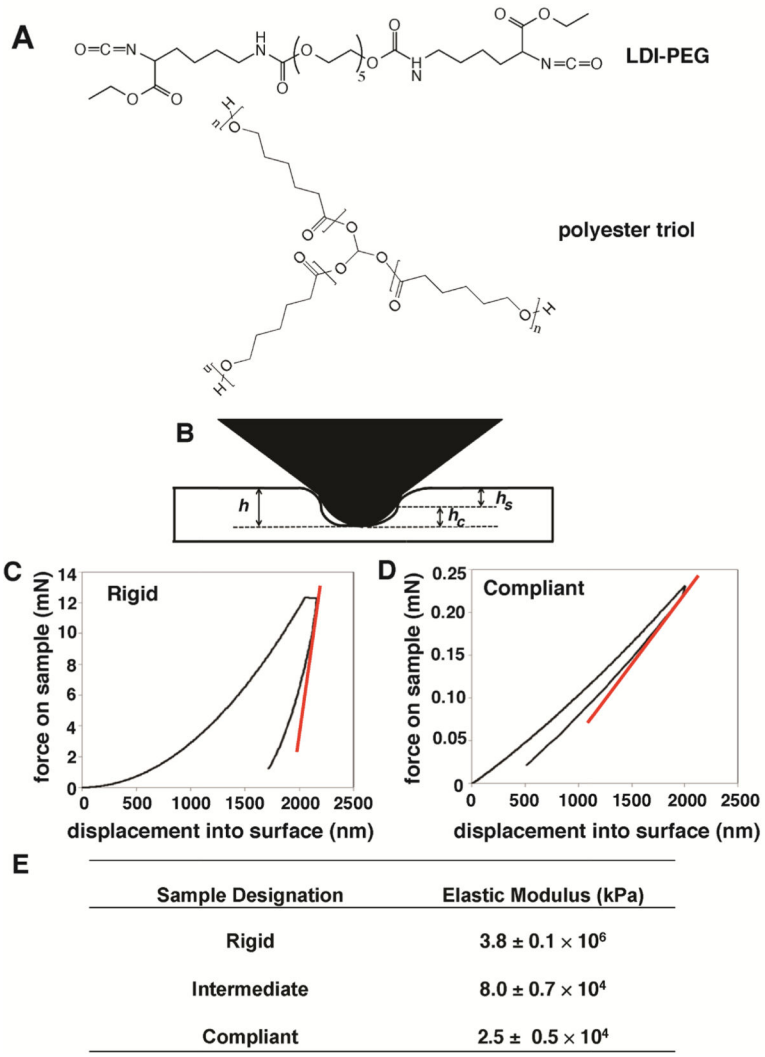

E

Sample Designation	Elastic Modulus (kPa)
Rigid	$3.8 \pm 0.1 \times 10^6$
Intermediate	$8.0 \pm 0.7 \times 10^4$
Compliant	$2.5 \pm 0.5 \times 10^4$

Figure 1.

(A) A lysine diisocyanate (LDI)-polyethylene glycol (PEG) prepolymer is reacted with a polyester triol to form a poly(ester urethane) network. (B) Diagram of the interaction between the nanoindenter and the sample. (C-D) Representative nanoindentation curves for rigid (C) and compliant (D) PUR films. Tangent curve (red) represents slope of the unloading curve required to obtain modulus data. (E) Table of measured modulus values for rigid, intermediate, and compliant polyurethane substrates.

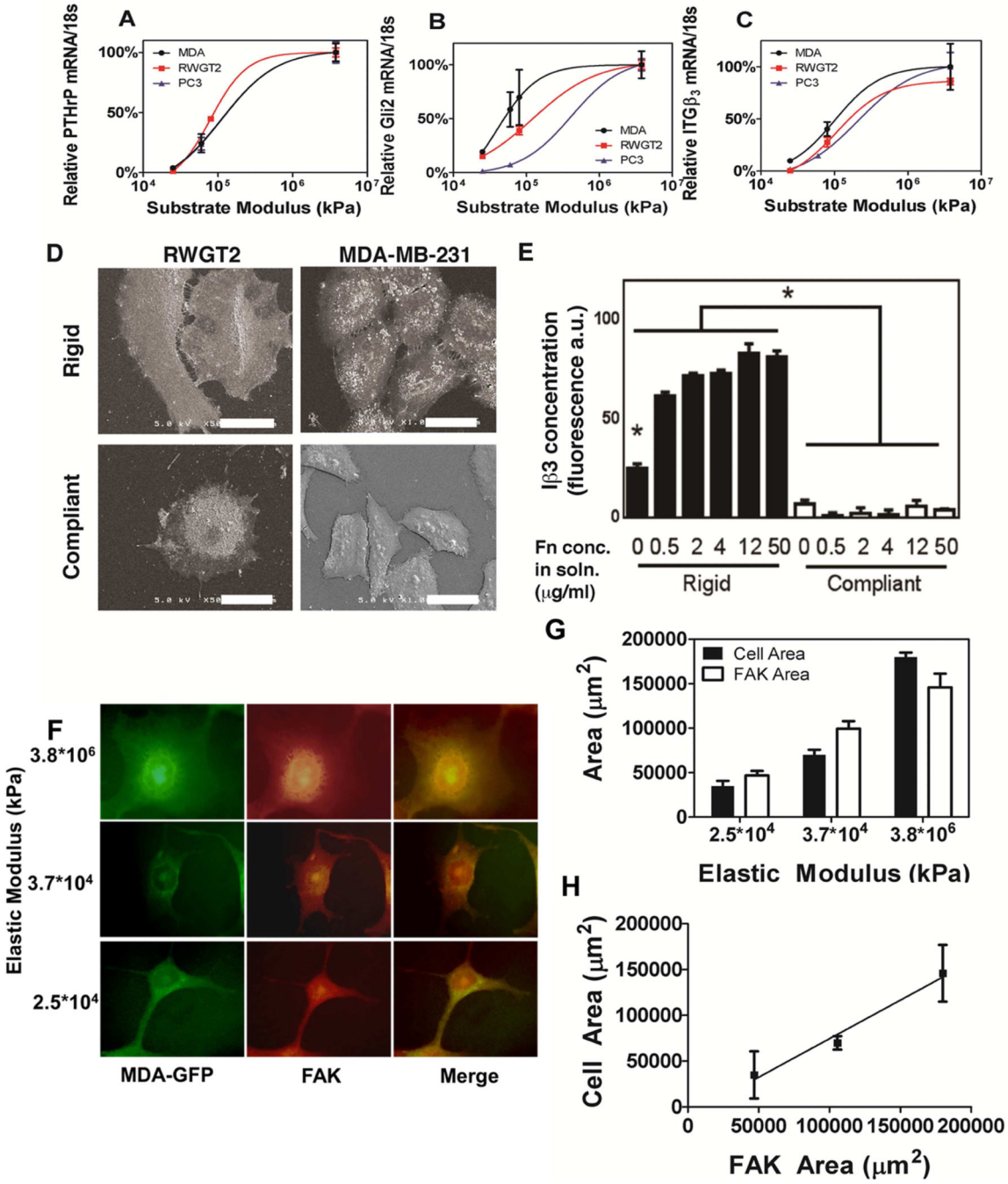

Figure 2.

Effect of changing rigidity on phenotype and gene expression. Gene expression of *PTHrP* (A), *Gli2* (B) and *Iβ3* (C) for MDA-MB-231 cells (black), RWGT2 cells (red), and PC3 cells (blue) seeded on polyurethane films of increasing rigidity. The lines are derived from a sigmoidal fit of the data completed with GraphPad (R^2>0.95 for all curves, *, p<0.05 to compliant). (D) Scanning electron micrographs of RWGT2 (scale bar = 60 μm) and MDA-MB-231 (scale bar = 30 μm) cells cultured on rigid and compliant films, where the cells show a more spread phenotype on rigid films. (E) Expression of *Iβ3* measured by

immunofluorescence as a function of rigidity and Fn concentration (*, $p<0.05$ rigid vs compliant; †, $p<0.05$ compared to all other rigid values). (F) 100× Immunofluorescent images of MDA-MB-231-GFP cells labeled with anti-focal adhesion kinase (FAK). (G-H) Quantification of FAK area and cell area with respect to rigidity. N=3 biological replicates

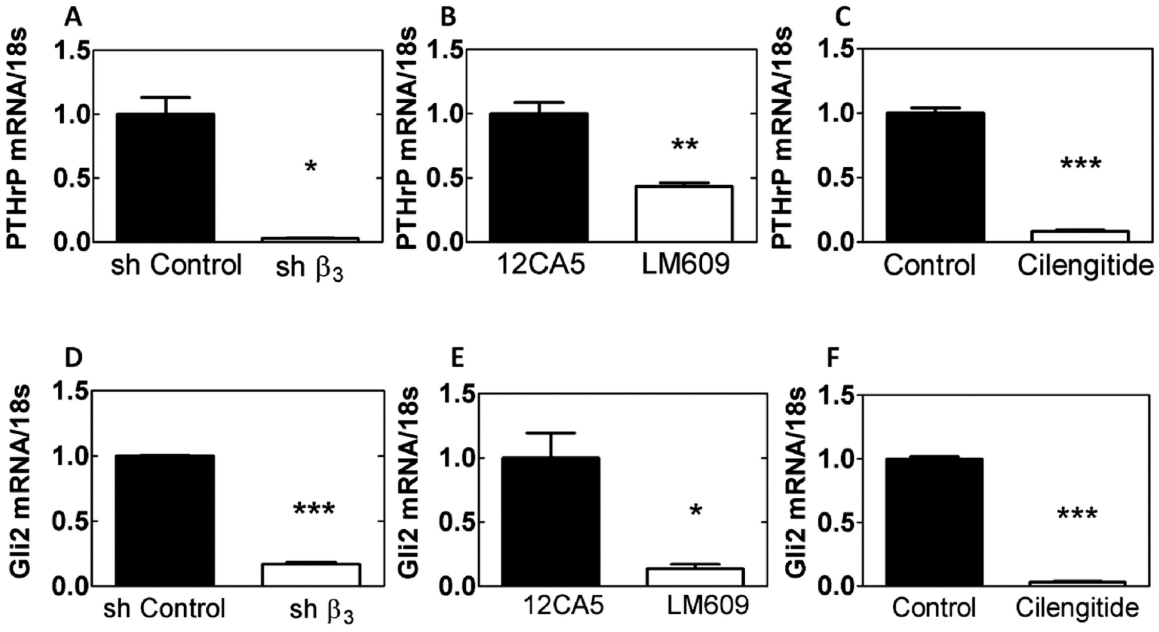

Figure 3.

Effects of genetic or molecular inhibition of $I\beta_3$ subunit. *PTHrP* and *Gli2* mRNA are significantly reduced when *Iβ3* subunit is knocked down with a targeted shRNA for integrin-β3 (A, D), the integrin specific antibody, LM609 (B, E), or an RGD-mimicking peptide Cilengitide (C, F) in normal serum media (* $p<0.05$, ** $p<0.01$, *** $p<0.005$). N=3 biological replicates. Data presented as fold change over MDA-MB-231 ctrl.

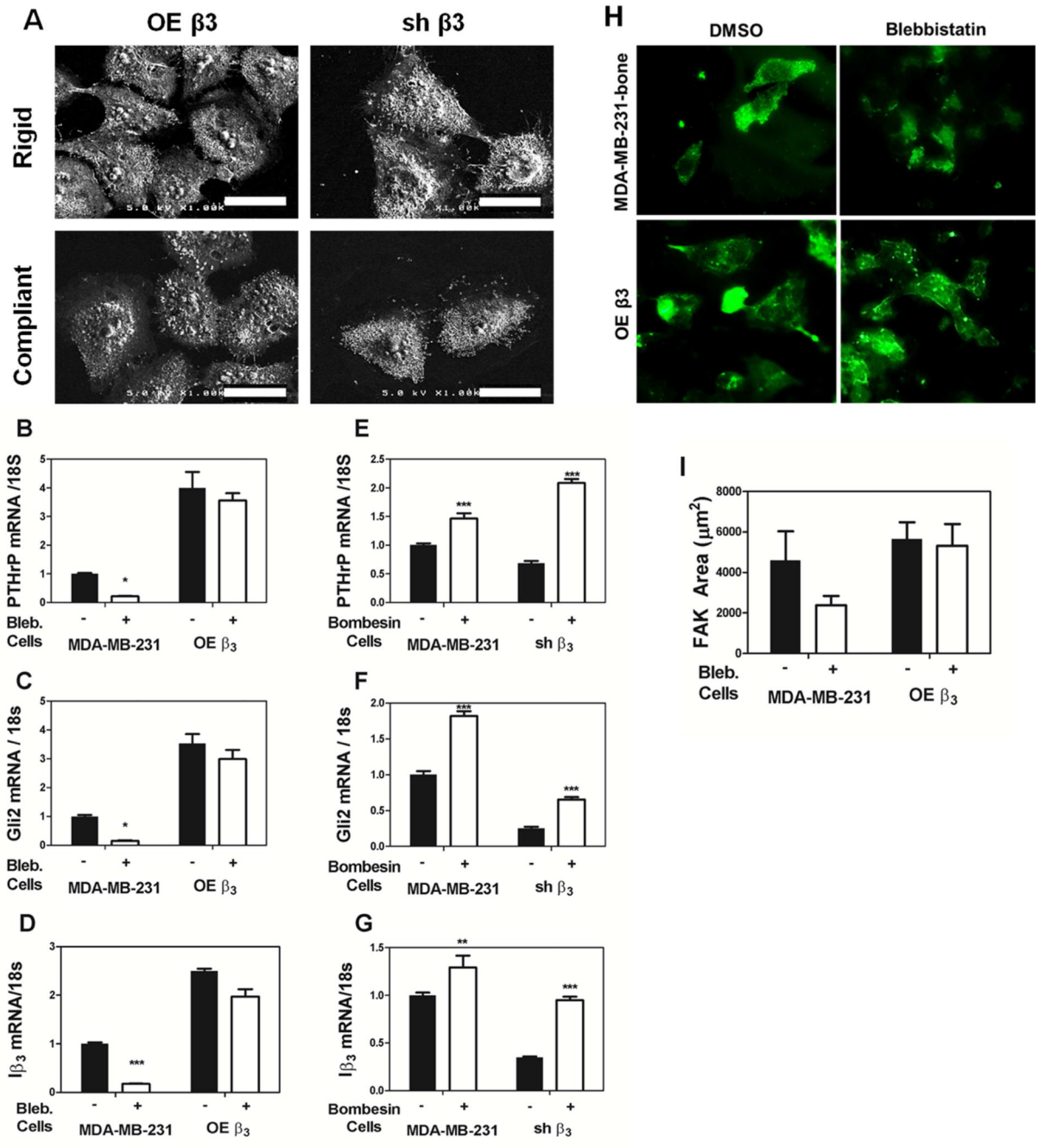

Figure 4.

Effects of *Iβ3* expression and downstream signaling on *PTHrP* and *Gli2* mRNA production. (A) Scanning electron microscopy (SEM) images of transfected MDA-MB-231 cells on rigid and compliant films demonstrate phenotypic changes regardless of the rigidity of the substrate (Scale bars = 60 μm). The OE β3 cells are highly spread on either film, while the shβ3 cells are more condensed on either film. MDA-MB-231 cells stably transfected to overexpress integrin β3 (OE β3 cells) treated with blebbestatin showed no difference in gene expression of *PTHrP*, *Gli2*, and *Iβ3* while blebbistatin treatment of the non-transfected

MDA-MB-231 cells significantly decreased *PTHrP* and *Gli2* (B-D). MDA-MB-231 cells and shβ3 cells treated with bombesin show a significant increase in *PTHrP*, *Gli2*, and *Iβ3* (E-G). (H) Immunofluorescent images MDA-MB-231-bone cells or OE β3 cells stained for focal adhesion kinase (FAK) show no significant change in FAK area (I). (* $p<0.05$. ** $p<0.01$, *** $p<0.005$). N=3 biological replicates. Data presented as fold change over untreated MDA-MB-231.

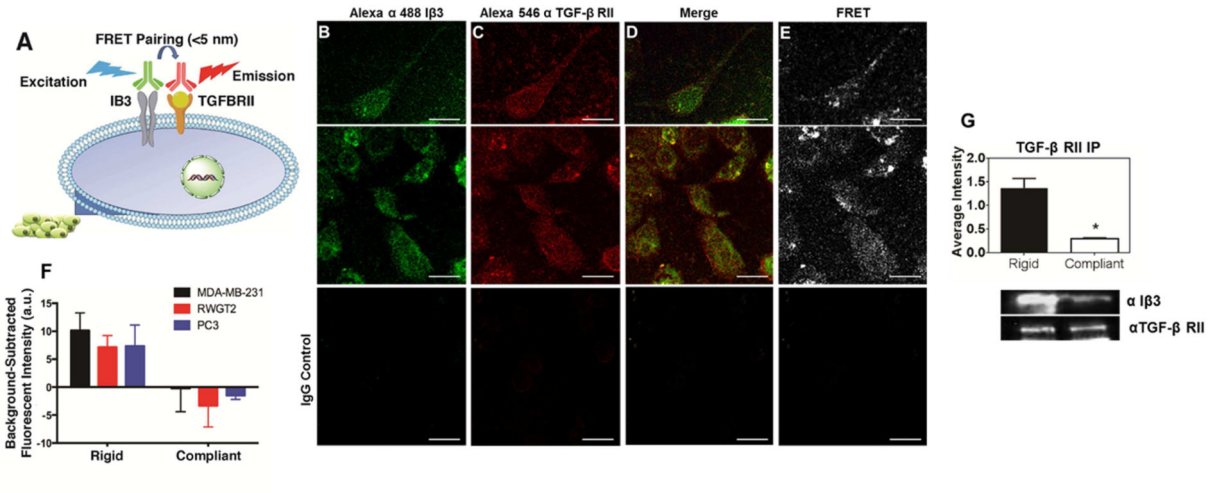

Figure 5.

Proximity of TGF-β RII and Iβ3 in MDA-MB-231 cells. (A) Schematic diagram of Förster resonance energy transfer (FRET) experiment. (B-E) 40× confocal images of cells stained with a fluorescently labeled antibody for Iβ3 subunit (Alexa 488; B), and TGF-β RII (Alexa 546; C) show colocalization (D) and a FRET response (E) of the two proteins. IgG control images show little fluorescent signal. (Scale bar = 50 μm). (E) Quantification of the FRET response of the two fluorescent antibodies reveals a significant increase of FRET expression on rigid PUR films indicating close proximity of TGF-β RII and Iβ3 subunit on the cell membrane for both MDA-MB-231-bone (black), RWGT2 (red), and PC3 cells (blue) *p<0.05. (F) Immunoprecipitation of TGF-β RII shows an association between Iβ3 and TGF-β RII on rigid surfaces.

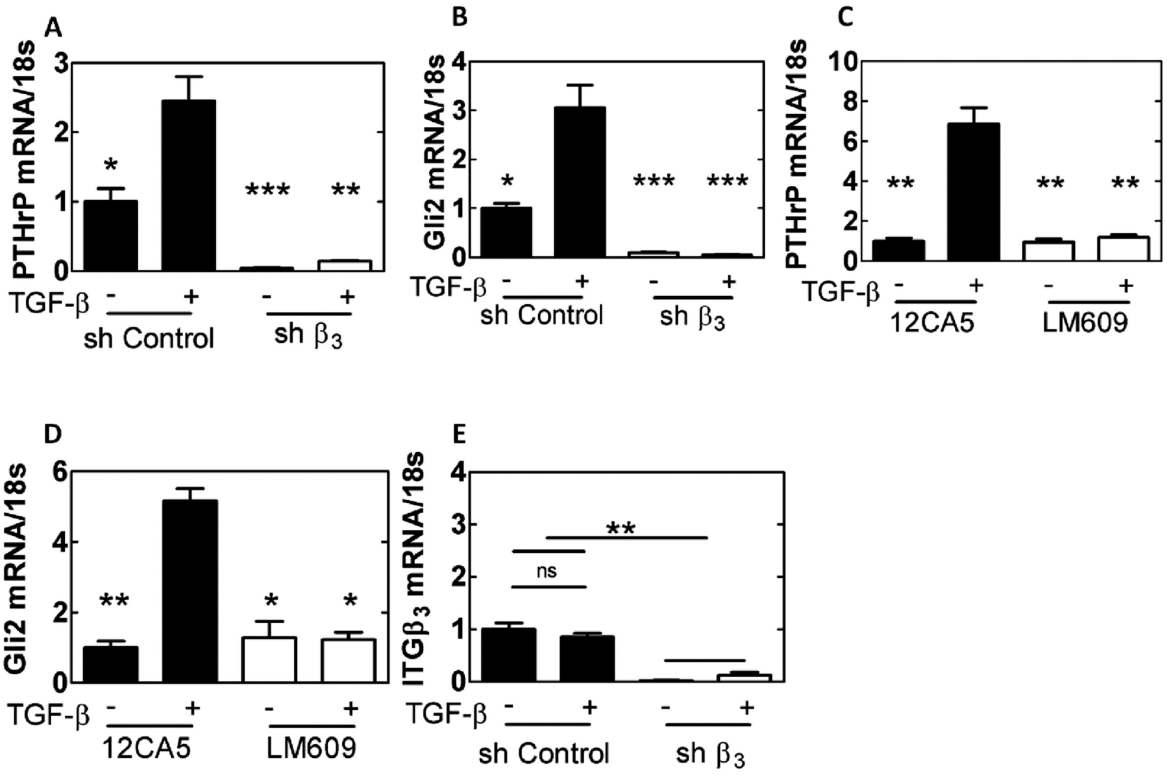

Figure 6.

Effects on TGF-β stimulation of genetic or molecular inhibition of Iβ3. *PTHrP* and *Gli2* levels are significantly reduced when Iβ3 subunit is knocked down with a targeted shRNA for integrin-β3 (A-B) or the integrin specific antibody LM609 (C-D) even in the presence of exogenous TGF-β. *Iβ3* is not affected by exogenous TGF-β (E). (* $p<0.05$, ** $p<0.01$, *** $p<0.005$). N=3 biological replicates. Data presented as fold change over untreated MDA-MB-231.

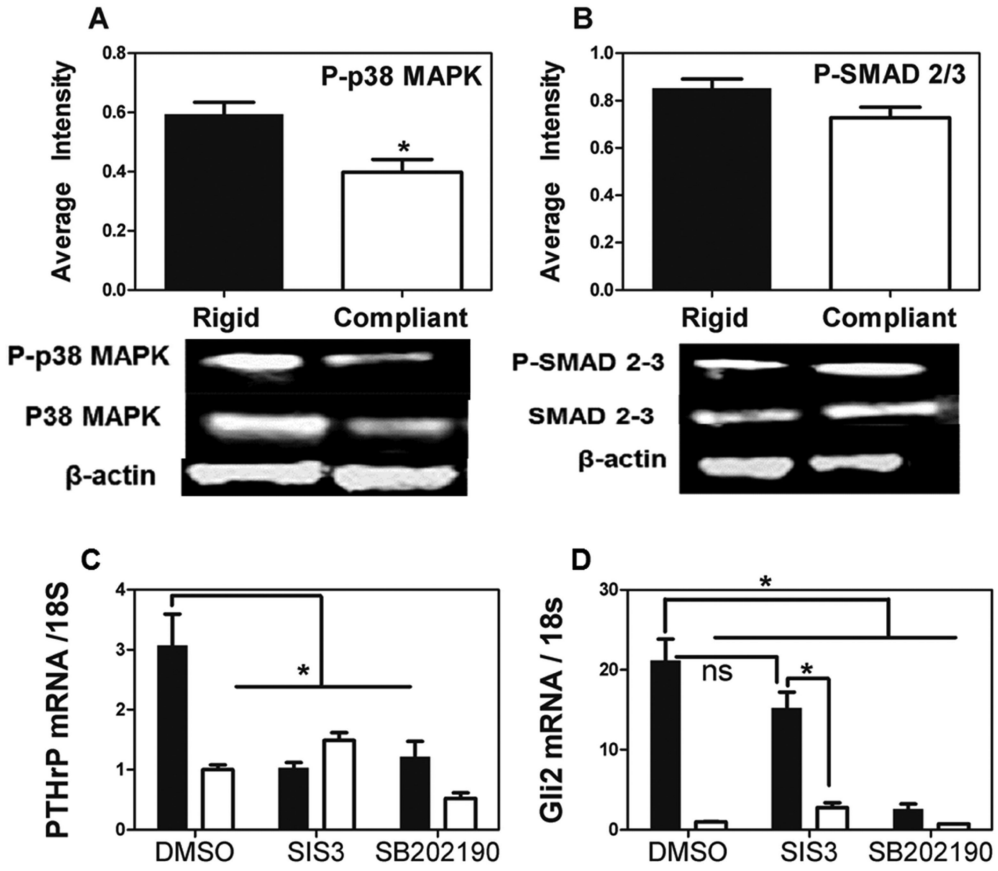

Figure 7.

Effects of substrate rigidity and TGF-β signaling on expression of *Gli2* and *PTHrP*. (A-B) Western blots of MDA-MB-231 cells seeded on rigid (black) and compliant (white) polyurethane films show an increase of activated Phospho-p38 MAPKα on rigid surfaces (A) while there were no significant differences in the SMADs (B). (C-D). Western blots were quantified by normalizing the band intensity of phosphorylated protein to total protein. MDA MB-231 cells were grown on rigid (black) or compliant (white) polyurethane films, treated with a SMAD inhibitor (SIS3) or a MAPK inhibitor (SB202190), and given exogenous TGF-β. SB202190 significantly reduced TGFβ stimulation of *PTHrP* (C) and *Gli2* (D) mRNA expression on rigid surfaces, while SIS3 significantly reduced TGFβ stimulation of *PTHrP* (C) but not *Gli2* (C) mRNA expression (* $p<0.05$). N=3 biological replicates. Data presented as fold change over untreated MDA-MB-231.

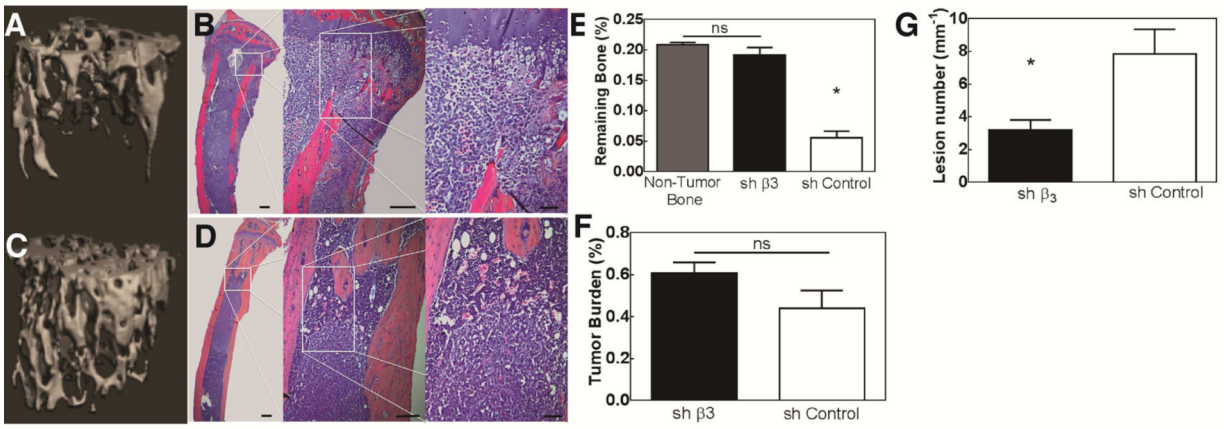

Figure 8.

Genetic inhibition of *Iβ3* in MDA-MB-231 cells transplanted into the tibia of immunocompromised mice. μCT reconstructions and histological sections of bone treated with control cells (A-B) and *Iβ3* knockdown cells (C-D) significantly decreased bone destruction, which is mirrored in the quantified bone volumes (E). Histological analysis showed that the tumor is present in both control and shβ3 cells (F); however, the tumor is shifted to the marrow and there is little bone destruction in the shβ3 cells (E-G). Quantified histomorphometry shows no significant difference in tumor burden between control and shβ3 cells (F). Additionally, quantification of lesion numbers from x-ray scans (G) show a reduced number of osteolytic lesions in the animals implanted with shβ3 cells (* $p<0.05$).

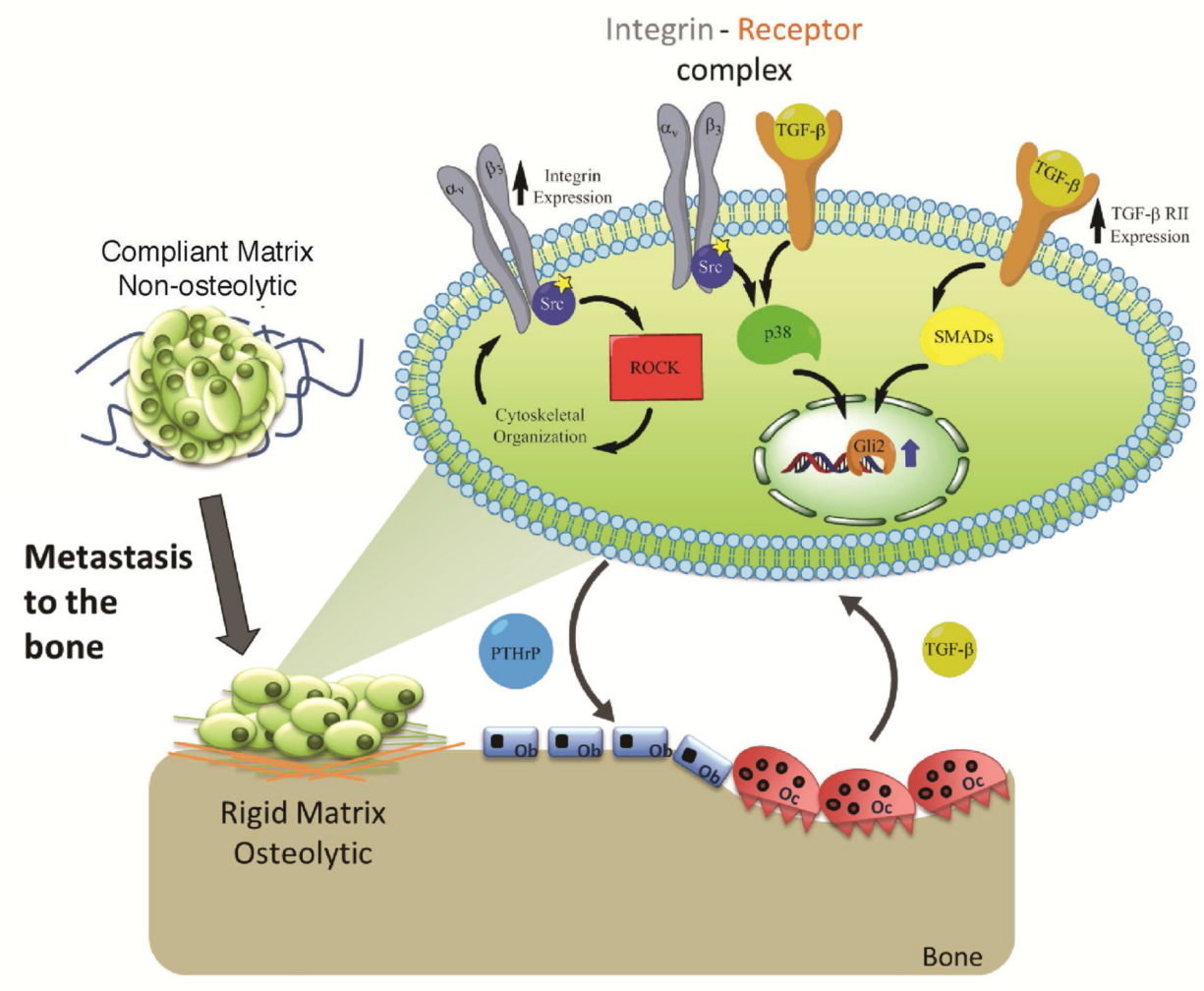

Figure 9.

Schematic diagram of the potential crosstalk of solid state (integrin) and soluble (TGF-β) signaling pathways that drive osteolytic behavior in metastatic bone cancer cells.